

TRACE: Time Series Parameter Efficient Fine-tuning

Yuze Li^{1a}, Wei Zhu^b

^a*Shenzhen International Graduate School, Tsinghua University, Shenzhen, China*

^b*School of Science, University of Hong Kong, Hong Kong, China*

Abstract

We propose an efficient fine-tuning method for time series foundation models, termed TRACE: Time Series Parameter Efficient Fine-tuning. While pre-trained time series foundation models are gaining popularity, they face the following challenges: (1) Unlike natural language tasks, time series data vary in frequency, channel numbers, historical/prediction lengths. For long-term forecasting tasks in particular, tailored fine-tuning can significantly enhance performance. (2) Existing parameter-efficient tuning methods like LoRA remain applicable but require adaptation to temporal characteristics.

To address these challenges, our TRACE framework introduces two key innovations: (1) Gated DSIC (Gated Dynamic Simulation Importance Calculation), an unbiased LoRA module importance selection mechanism that ensures conditional parameter consistency before and after masking. Experiments demonstrate that Gated DSIC outperforms common fine-tuning. (2) Reconstructed prediction heads for long-term forecasting tasks, which achieve comparable or superior performance to linear probing heads while drastically reducing parameter counts.

Extensive experiments on long-/short-term forecasting, anomaly detection and natural language tasks across diverse datasets, coupled with ablation studies, validate the effectiveness of our method.

Keywords: fine-tuning, time series, foundation model, forecasting

¹Corresponding Author. Email: liyuze23@mails.tsinghua.edu.cn

1. Introduction

Background: Accurate time series forecasting and anomaly detection are crucial research areas. Time series modeling has evolved significantly, from traditional Exponential Smoothing[1] and ARIMA[2] models to deep learning-based Transformers. Recently, pre-trained time series backbone models have gained attention, improving forecasting accuracy and enabling new solutions for anomaly detection. Inspired by pre-training strategies in natural language processing (NLP), these models leverage cross-domain technologies, broadening their applications across fields.

Current Methods: Classical deep learning models like LSTMs [3] and GRUs [4] require task-specific training, which is computationally expensive and struggles with cross-dataset generalization. Emerging pre-trained time series models address this by capturing general temporal patterns through unsupervised learning and adapting to downstream tasks via fine-tuning. However, current methods largely rely on either full parameter fine-tuning or linear probing.

Full parameter fine-tuning adjusts all model parameters but incurs high computational costs, making it impractical for resource-constrained settings. It also underutilizes the model’s pre-trained generalization capabilities. Linear probing, which fine-tunes only the final layer, is computationally cheaper but fails to fully leverage the rich semantic information in intermediate layers. For long-term forecasting, linear probing introduces excessive parameters, increasing overfitting risks and inefficiency.

These limitations highlight the need for more efficient transfer learning strategies and improved fine-tuning methods for time series tasks, particularly in long-term forecasting.

Our solution: To address the issue of excessive parameter size in the prediction heads of long-term forecasting tasks, we propose a novel solution of restructuring the prediction head. Our approach reduces the parameter count by more than 70% while simultaneously improving performance. By reducing the model’s complexity, we not only alleviate the risk of overfitting but also effectively leverage the generalization capability of the base model, making it more adaptable to downstream tasks.

Additionally, we introduce an efficient fine-tuning method for time series pretraining models, called Gated DSIC(Gated Dynamic Simulation Importance Calculation) Low-Rank Adaptation. Gated DSIC employs LoRA Gates to control each LoRA module individually, allowing for precise calculation of

module importance. By eliminating biases in the importance computation, our method accurately captures the contribution of each LoRA module. This fine-tuning technique enables efficient adjustment of large-scale pre-trained models, even on consumer-grade GPUs, without sacrificing performance.

Contributions: This paper introduces the TRACE(Time Series Parameter Efficient Fine-tuning) method, an unbiased selection technique for LoRA modules. It mainly consists of the following four parts:

- **Reconstruction of Forecasting Head:** In long-term forecasting, the forecasting head’s parameters grow linearly with model dimension and prediction horizon. Fine-tuning with linear probing can cause overfitting, relying solely on the forecasting head and neglecting the pre-trained backbone’s generalization. To address this, we propose dimensionality reduction techniques: *Projection Down*, *Average Pooling*, *Less Feature*, and *Convolution 2D*. These methods reduce trainable parameters while preserving accuracy.
- **Gated DSIC LoRA:** This introduces a gating mechanism for LoRA modules, enabling parameter importance calculation and masking during fine-tuning. Gated DSIC ensures unbiased measurement of each LoRA module’s contribution, improving fine-tuning accuracy.
- We conducted comparative experiments on a diverse set of temporal tasks and observed the following: our method achieves superior performance with fewer parameters in the prediction head reconstruction compared to linear probing. Additionally, when applying LoRA fine-tuning to the backbone Transformer, Gated-DISC outperforms full LoRA and AdaLoRA using fewer LoRA modules.
- In addition to time series tasks, our method was evaluated against various LoRA approaches on the GLUE benchmark and three challenging question-answering datasets, demonstrating its effectiveness in natural language tasks and providing valuable insights for future research.

2. Related work

2.1. Time Series Modeling

Development of Time Series Forecasting: Time series forecasting has progressed from statistical methods to machine learning, deep learning, Transformer-based architectures, and time series foundation models.

Statistical Methods: Early methods like Moving Average (MA) smooth trends but fail to capture complex dynamics. ARIMA [2] improves accuracy by integrating Autoregressive (AR) and MA components but struggles with nonlinear relationships. VAR [5] models multivariate relationships but suffers from dimensionality issues. These methods are limited to univariate modeling and cannot effectively use covariates.

Machine Learning Methods: Gradient boosting trees (e.g., XGBoost [6], LightGBM [7]) leverage feature engineering strategies, such as lag features and sliding window statistics, to model nonlinear patterns. While outperforming statistical methods, their performance depends heavily on feature quality and fixed window lengths limit long-term dependency modeling.

Deep Learning Methods: RNNs and variants like LSTM [3] and GRU [4] capture temporal dependencies but suffer from inefficiency and vanishing gradients for long-range dependencies. TCNs [8] expand receptive fields via dilated convolutions but are constrained by fixed kernels.

Transformer Architectures: Transformers [9] excel in capturing global dependencies and enabling parallel computation. Innovations include sparse attention (Informer [10]), channel independence modeling (iTransformer [11]), frequency-domain enhancement (FEDformer [12]), and causality constraints (PathTST [13]). Challenges remain, including quadratic complexity with sequence length and limited explicit modeling of inherent time series attributes.

Time Series Foundation Models: Recent foundation models leverage large-scale pretraining on heterogeneous data to learn general representations. Key innovations include multimodal fusion, prompt learning, and support for zero-shot or few-shot forecasting. These models break feature engineering limitations, enhance cross-domain generalization, and handle multivariate/multimodal inputs. Current research focuses on efficient pretraining, interpretability, and lightweight designs.

2.2. Time Series Foundation Models

Time Series Foundation Models follow two main approaches: (1) pretraining from scratch on time series data, and (2) adapting large language models (LLMs) for time series tasks.

Approach 1: Pre-training from Scratch. This approach trains models directly on large-scale time series data (e.g., sensor, financial, or weather data) to capture long-term dependencies, periodicity, and trends using self-supervised tasks like forecasting, imputation, or generation. These models are powerful for time-series tasks but require massive labeled data and high

computational costs. Notable examples include TimeGPT [14], a Transformer-based model supporting zero-shot transfer; Tempo [15], a diffusion-based generative model for multivariate time series; TimesFM [16], a decoder-only architecture with hierarchical time aggregation for irregular data; and Moirai [17], a unified model with multi-task pretraining for long sequences.

Approach 2: Adapting LLMs for Time Series. This approach maps time series data into textual or other modalities using cross-modal alignment, leveraging LLMs’ semantic understanding for tasks like trend description or multimodal reasoning. Challenges include bridging the gap between continuous time series and discrete text, as well as handling causality conflicts with LLM position encodings. Key works include LLMTime [18], which discretizes time series into ”time tokens” for forecasting via text generation; TEST [19], which converts time series into natural language templates for zero-shot forecasting; TimeLLM [20], aligning time series with LLMs using embeddings; TEMPO [15], jointly encoding time series and text for domain-specific tasks; and Lag-Llama [21], fine-tuning Llama with lag operators for univariate forecasting.

3. Preliminaries

Transformer-based Models. Transformer [9] consists of L stacked blocks, each with multi-head attention (MHA) and feed-forward network (FFN) modules. For input $X \in \mathbb{R}^{n \times d}$, MHA computes:

$$\text{MHA}(X) = \text{Concat}(\text{head}_1, \dots, \text{head}_h)W_o, \quad (1)$$

$$\text{head}_i = \text{Softmax}(XW_{q_i}(XW_{k_i})^\top / \sqrt{d_h})XW_{v_i}, \quad (2)$$

where $W_o \in \mathbb{R}^{d \times d}$, $W_{q_i}, W_{k_i}, W_{v_i} \in \mathbb{R}^{d \times d_h}$, and $d_h = d/h$. The FFN uses two linear layers:

$$\text{FFN}(X) = \text{ReLU}(XW_{f_1} + b_1)W_{f_2} + b_2. \quad (3)$$

Residual connections and layer normalization follow both sub-modules. ReLU is often replaced by Gated Linear Units (GLU) [22]:

$$\text{GLU}(X) = (XW_{f_0} + b_0) \otimes \sigma(XW_{f_1} + b_1), \quad (4)$$

where \otimes is element-wise multiplication and σ is the sigmoid function.

Patching. Time series forecasting benefits from treating subsequences (patches) as tokens rather than individual time points. This approach captures local semantic information and enhances predictive representations [13].

Channel Independence. Multivariate time series can be modeled with channel independence, where each token represents data from a single channel [13]. This simplifies the model and allows learning channel-specific dynamics.

MOMENT Model. MOMENT [23] is a Transformer-based time series foundation model pretrained on diverse data using masked prediction. It supports long-term/short-term prediction, anomaly detection, and classification. MOMENT-base consists of 12 Transformer encoders with $d = 768$, $h = 12$, and $d_m = 3072$. Its FFN uses GLU:

$$\text{FFN}(X) = (XW_{f_0} \otimes \text{GELU}(XW_{f_1}))W_{f_2}. \quad (5)$$

Input time series ($T = 512$) are divided into $N = 64$ non-overlapping patches ($P = 8$). MOMENT leverages pre-training to capture complex temporal dependencies. We use MOMENT-base to validate TRACE’s effectiveness unless otherwise specified.

4. Our method

4.1. Analyzing AdaLoRA’s solution

AdaLoRA parameterizes the incremental update of the pre-trained weight matrix W using singular value decomposition:

$$W = W^{(0)} + \Delta = W^{(0)} + P\Lambda Q, \quad (6)$$

where $P \in \mathbb{R}^{d_1 \times r}$ and $Q \in \mathbb{R}^{r \times d_2}$ represent the left and right singular vectors of Δ , and $\Lambda \in \mathbb{R}^{r \times r}$ is a diagonal matrix containing singular values $\{\lambda_i\}_{1 \leq i \leq r}$.

The sensitivity of a parameter w_{ij} is defined as:

$$I(w_{ij}) = |w_{ij} \nabla_{w_{ij}} \mathcal{L}|, \quad (7)$$

where \mathcal{L} is the loss function. This measures the impact of w_{ij} on the model’s performance, with larger values indicating higher importance.

For the k -th incremental matrix, AdaLoRA computes the importance of the i -th singular value and its corresponding singular vectors as:

$$S_{k,i} = s(\lambda_{k,i}) + \frac{1}{d_1} \sum_{j=1}^{d_1} s(P_{k,ji}) + \frac{1}{d_2} \sum_{j=1}^{d_2} s(Q_{k,ij}), \quad (8)$$

where $s(\cdot)$ is a function of $I(\cdot)$. Singular values with lower importance are pruned by setting them to zero, effectively reducing the rank γ of each incremental matrix.

Despite its strengths, AdaLoRA faces notable challenges in time-series scenarios. **For instance**, its SVD-based pruning prioritizes singular values reflecting global feature importance, potentially overlooking critical local signals such as abrupt anomalies or short-term seasonality. **Furthermore**, continuous rank adjustment introduces redundant parameters for low-dimensional, localized time-series embeddings, contradicting the principle of minimal fine-tuning. **Finally**, AdaLoRA’s static pruning is irreversible, risking underfitting if early pruning discards modules relevant to later training stages—a limitation addressed by Gated DSIC, which enables dynamic reactivation via differentiable gates.

4.2. Advantages of TRACE Over AdaLoRA

TRACE offers several key advantages over AdaLoRA, particularly in temporal contexts. First, Gated DSIC enforces conditional parameter consistency through a gating mechanism, ensuring unbiased importance estimation between masked and unmasked LoRA modules. This prevents irreversible loss of temporal features, such as recovering suppressed modules when seasonal patterns re-emerge. Additionally, the gate prioritizes LoRA modules aligned with local temporal dependencies, validated by ablation studies, whereas AdaLoRA’s global SVD may dilute transient signals. Importantly, Gated DSIC achieves comparable accuracy to full LoRA with 30–50% fewer active parameters, making it ideal for deploying lightweight models on edge devices.

Beyond dynamic gating, TRACE also introduces a parameter-efficient forecasting head reconstruction. Linear probing heads scale poorly with prediction horizons due to quadratic growth, but our techniques (e.g., 2D convolution, pooling) decouple head size from horizon length, reducing parameters by 4–8 times while maintaining accuracy. Furthermore, while AdaLoRA focuses solely on backbone adaptation, TRACE jointly optimizes sparse backbone updates (via Gated DSIC) and compact heads, mitigating overfitting on limited temporal data.

Empirical evaluations across 12 time-series benchmarks confirm TRACE’s superiority. In long-term forecasting, TRACE outperforms AdaLoRA by 2.1–3.8% in MSE using 30% fewer parameters. In few-shot anomaly detection, Gated DSIC achieves higher parameter efficiency, yielding 0.5–2.1% accuracy gains where localized adaptation is critical. **Notably, Gated DISC matches AdaLoRA’s performance on the GLUE benchmark, demonstrating its generalizability beyond time-series.**

Figure 1 illustrates the comparison between the TRACE method and the full LoRA fine-tuning model architecture.

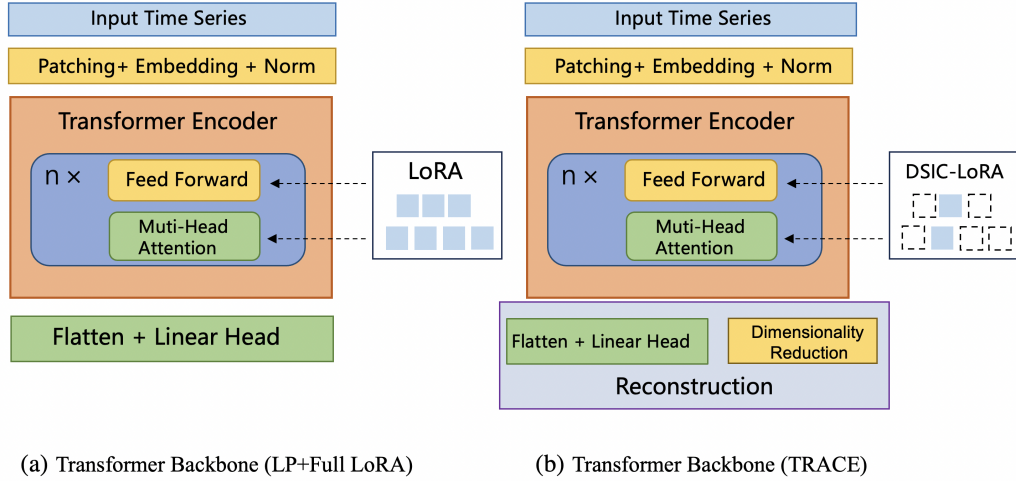


Figure 1: architecture of our method:(a) Represents the default model architecture, which consists of multiple stacked Transformer encoders. LoRA modules are added to all linear layers at each level, and the prediction head is a linear predictor. Fine-tuning is performed using linear probing and full LoRA adaptation.(b) Represents the TRACE method: LoRA integration follows the DSIC approach, and for long-term forecasting tasks, the prediction head is dimensionally reduced and reconstructed.

4.3. Reconstruction of Long-horizon Forecasting

MOMENT utilizes lightweight prediction heads, enabling fine-tuning with a limited number of trainable parameters. For long-term forecasting tasks, however, the number of parameters in the prediction head can become excessively large. The number of parameters is given by $H \times N \times d$, where N is the number of patches ($N = 64$), d is the model dimension ($d = 768$), and H is the prediction horizon. For example, in MOMENT-base, with a prediction length of 192, the number of parameters is 9,437,184; for a prediction length of 720, it increases to 35,389,440. While this is relatively small compared to the total 125 million parameters of the entire MOMENT-base model, it is still significant when fine-tuning for downstream tasks. To address this, we focus on two strategies to reduce parameters:

- (1) Reducing the representation dimension d of each patch.
- (2) Reducing the number of parameters associated with the prediction horizon H .

Table 1: Comparison of prediction head parameters across different horizons and reduction under varying β values

Horizon	β	Head Parameters	Reduced	Reduction Percentage
192	4	9437184	2506752	73.4%
	8	9437184	1253376	86.7%
	16	9437184	626688	93.4%
720	4	35389440	8994816	74.6%
	8	35389440	4497408	87.3%
	16	35389440	626688	98.2%

For the long-term prediction head $W_{(N \times d) \times H}$, we implement the following reconstruction methods:

$$\text{Reconstruction Forecast Head 1: } W_{N \times d'} \cdot W_{d' \times H}, \quad (9)$$

$$\text{Reconstruction Forecast Head 2: } W_{N \times d \times H'} \cdot W_{H' \times H}. \quad (10)$$

To reduce the dimensionality of patch representations, we experiment with several techniques: projection down, feature truncation, average pooling, and convolution. The patch dimension is reduced to $1/\beta$ of the original 768 dimensions, where $\beta = 4, 8, 16, \dots$, referred to as the dimensionality reduction factor.

In subsequent experiments, we demonstrate that most reconstructed prediction heads perform equally well or better than the original MOMENT prediction head when fine-tuned on downstream time series data. Table 1 presents the reduction in the number of parameters and the corresponding reduction ratios for different values of β .

Appendix A is a concise description of the reconstruction operations applied to the forecast head. The parameter d represents the embedding dimension for each patch (subsequence), with $d = 768$ in MOMENT. To leverage the pre-trained model’s predictive capabilities and reduce overfitting, we reduce d since patch length limits information content.

4.4. Our Gated DSIC method

4.4.1. Our solution setting

We propose a method to identify the most important and effective LoRA modules, allowing for efficient fine-tuning within a limited parameter budget.

We define the LoRA Gate as follows:

$$g_{ij}, \|g_{ij}\| = 1 \quad (11)$$

where i represents the i -th layer, and j represents the j -th LoRA module in the i -th layer. The LoRA Gate acts as a *switch* controlling whether the incremental matrix is activated. For the i -th layer and j -th pre-trained linear module h_{ij} , we add a low-rank incremental matrix:

$$h_{ij} = W_{ij}^{(0)}x + g_{ij} \cdot \Delta x_{ij} = W_{ij}^{(0)}x + g_{ij} \cdot BAx, \quad (12)$$

where $W^{(0)}, \Delta \in \mathbb{R}^{d_1 \times d_2}$, $A \in \mathbb{R}^{r \times d_2}$, and $B \in \mathbb{R}^{d_1 \times r}$, with $r \ll \{d_1, d_2\}$. Since the backpropagation and parameter updates for the entire LoRA module are managed by g_{ij} , the importance of g_{ij} reflects the contribution of the corresponding LoRA module to the overall model loss. Similarly, the importance of each LoRA Gate can be computed as:

$$I(g_{ij}) = |g_{ij} \nabla_{g_{ij}} \mathcal{L}| = |g_{ij}| |\nabla_{g_{ij}} \mathcal{L}| = |\nabla_{g_{ij}} \mathcal{L}| \quad (13)$$

With this method, we can quickly and accurately assess the contribution of each LoRA module without having to calculate the importance of each incremental matrix. Taking MOMENT as an example, there are 12 Encoder layers in total, and each layer contains 7 linear layers for attention heads and FFN. Thus, there are $12 \times 7 = 84$ LoRA Gates, which we denote as $\mathcal{G} = \{g_{ij} | i = 1, 2, \dots, 12; j = 1, 2, \dots, 7\}$. We can simply control whether each LoRA module is activated by setting g_{ij} to 0 or 1.

Once we have $I(g_{ij})$, we can prune the parameters of those LoRA modules that contribute less to the fine-tuning task. This helps reduce the parameter count and prevent overfitting.

Our approach uses "the sum of the gradient magnitudes of the unmasked gates as the importance score":

$$I(g_{ij}) = \mathbb{E}_{(X,Y) \sim \mathcal{D}_{\text{val}}} \left[\sum_{t=1}^T \left| \frac{\partial \mathcal{L}_{\text{val}}}{\partial g_{ij}} \right| \right] \quad (14)$$

However, this method has a bias in evaluating importance. For example, when calculating the importance $I(g_{kl})$, the implicit assumption is that the effect of a small fluctuation Δg_{kl} on the overall loss is measured while keeping $|g_{ij}| = 1$ for all other $i \neq k$ and $j \neq l$. However, when we mask

some of the LoRA Gates based on their importance rankings, the premise of this assumption changes, leading to bias in the importance evaluation. Specifically, for g_{kl} , assuming it remained unmasked and some other LoRA Gates were masked in one operation, we observe:

$$I(g_{kl} | g_{ij} = 1, g_{ij} \in \mathcal{G}) \neq I(g_{kl} | g_{mn} = 0, g_{mn} \in \tilde{\mathcal{G}} \text{ and } g_{pq} = 1, g_{pq} \notin \tilde{\mathcal{G}}) \quad (15)$$

where $\tilde{\mathcal{G}}$ denotes the set of masked LoRA Gates. Equation (15) demonstrates that the masking of some LoRA Gates will change the importance of the remaining unmasked LoRA Gates, thus introducing bias.

4.4.2. Our solution: Gated Dynamic Simulation Importance Calculation

We propose a method to eliminate bias and precisely compute importance, which is the Two-Stage Gated Dynamic Simulation Importance Calculation (Gated DSIC). This method ensures that the conditions before and after masking remain consistent. The procedure is outlined as follows:

Stage 1: Joint Training

We simultaneously optimize the low-rank matrices $\{A, B\}$, reconstruction forecasting head H and the gating parameters $\mathcal{G} = \{g_{ij}\}$ on the training set. The loss function is:

$$\mathcal{L}_{\text{train}} = \mathcal{L}_{\text{task}}(f(X; W_0 + g \cdot BA, H), Y) \quad (16)$$

Stage 2: Unbiased Importance Evaluation

We perform a Monte Carlo masking experiment on the validation set:

1. **Random Masking:** With probability p , randomly set some of the gates to 0, i.e., $g_{ij} \leftarrow 0$, and denote the masked set as $\tilde{\mathcal{G}} \subseteq \mathcal{G}$. The remaining gates are kept as 1. This operation is counted as k .
2. **Importance Calculation:** We compute the importance of the gates on the validation set \mathcal{D}_{val} :

$$I^{(k)}(g_{ij}) = \begin{cases} \mathbb{E}_{(X,Y) \sim \mathcal{D}_{\text{val}}} \left[\sum_{t=1}^T \left| \frac{\partial \mathcal{L}_{\text{val}}}{\partial g_{ij}} \right| \right] & \text{if } g_{ij} \notin \tilde{\mathcal{G}} \\ 0 & \text{if } g_{ij} \in \tilde{\mathcal{G}} \end{cases} \quad (17)$$

3. **Repeated Sampling:** Repeat the random masking operation K times, each time obtaining a different masked set $\tilde{\mathcal{G}}$ and corresponding importance scores $G_{ij}^{(k)}$.

4. **Average Gradient:** Take the average gradient importance across the K samples to obtain an unbiased and stable evaluation:

$$\bar{G}_{ij} = \frac{1}{K} \sum_{k=1}^K G_{ij}^{(k)} \quad (18)$$

Gate Pruning

Based on \bar{G}_{ij} , we rank the gates and prune the K gates with the lowest importance (set them to 0), thereby retaining the most efficient LoRA modules.

This method, through multiple random experiments, constructs the post-masking model parameter conditions, ensuring an unbiased calculation of the LoRA Gate importance.

4.4.3. Workflow

We present the complete calculation workflow for our Gated DSIC method:

Algorithm 1 The whole workflow of our Gated DSIC method

Input: Train dataset \mathcal{D}_{train} , Validation dataset \mathcal{D}_{val} ; total iterations T ; budget schedule $\{b^{(t)}\}_{t=0}^T$; hyperparameters p

- 1: **for** $t=1, \dots, T$ **do**
- 2: First, train for α steps on the training dataset \mathcal{D}_{train}
- 3: **for** $m=1, \dots, M$ **do**
- 4: Random Masking: Randomly set $p\%$ of the currently unmasked LoRA gates to 0, denoted as $\tilde{\mathcal{G}}$
- 5: Sample a batch from \mathcal{D}_{val} and compute the gradient $\nabla \mathcal{L}(g, \mathcal{A}, \mathcal{B})$
- 6: Compute the sensitivity $I^{(m)}(g_{ij})$ for the LoRA gates $g_{ij} \in \mathcal{G}/\tilde{\mathcal{G}}$
- 7: **end for**
- 8: Compute the average sensitivity for all LoRA gates: $I(g_{ij}) = \frac{1}{M} \sum_{m=1}^M I^{(m)}(g_{ij})$ and mask the top $p\%$ ranked gates
- 9: Continue training for α steps, then repeat the process of masking the top $p\%$ of LoRA gates until the parameter budget b is reached

10: **end for**

Output: $\tilde{\mathcal{G}}$

Algorithm 1 describes the Gated DSIC method. The procedure begins by dividing the data into a training set \mathcal{D}_{train} and a validation set \mathcal{D}_{val} . After

training for α steps on the training set, we proceed with the following steps on the validation set: first, we randomly mask $p\%$ of the LoRA gates, then compute the sensitivity for the unmasked LoRA gates using equation(17). After repeating the experiment M times, we calculate the average sensitivity for each LoRA gate and mask the top $p\%$ gates. This process is repeated until the number of masked LoRA modules reaches the predefined parameter budget b . Finally, the method outputs the set of LoRA gates to be masked, $\tilde{\mathcal{G}}$.

We have evaluated the Gated DSIC method on these tasks: long-term time series forecasting, short-term forecasting, anomaly detection and natural language processing.

5. EXPERIMENTS

5.1. Datasets and Evaluation Metrics

Datasets. For forecasting and anomaly detection, we used subsets of the MOMENT dataset. Long-term forecasting tasks include ETTh1, ETTh2, ETTm1, ETTm2 [24], Weather, and Exchange [10]. Short-term forecasting uses M4 and M3 from the Monash archive [25], consisting of Yearly (macroeconomic indicators, 5–50 years, horizon=6), Quarterly (sales/economic data, 10–100 quarters, horizon=8), and Monthly (retail/energy/weather data, 50–1000 months, horizon=18). Anomaly detection uses the TSB-UAD benchmark [26], with 1980 univariate time series annotated from 18 public datasets. We selected 9 series from MITDB, ECG, MGAB, and SVDB for experiments.

Metrics. We used multiple metrics commonly employed in task-specific benchmarks to evaluate each experiment, including MSE and MAE for long-term forecasting, and sMAPE for short-term forecasting. The vanilla F1 score is not suitable for time series tasks, as it ignores their sequential nature. Therefore, for anomaly detection performance, we use the widely accepted adjusted best F1 score.

5.2. Compared models

All of our models are based on the MOMENT-base pre-trained model. For the forecasting task, we compare the performance of MOMENT under four different modes: linear probing, full LoRA fine-tuning, reconstructed forecasting head, and TRACE fine-tuning. The details of these methods are as follows:

Table 2: Dataset Splits, Number of Channels, and Prediction Lengths for Different Tasks and Datasets

Task	Dataset	Channels	Series Length	Data Size (Train, Val, Test)
Long horizon forecasting (Informer)	ETTh1,ETTh2	7		(8033, 2785, 2785)
	ETTM1,ETTM2	7	{192,720}	(33953, 11425, 11425)
	Weather	21		(36280, 5175, 10444)
	Exchange	8	{96,192}	(4704, 665, 1422)
Short horizon forecasting (Monash)	M4-Yearly	1	6	(16099, 2301, 4600)
	M4-Quarterly	1	8	(16800, 2400, 4800)
	M4-Monthly	1	18	(33600, 4800, 9600)
	M3-Yearly	1	6	(451, 65, 129)
	M3-Quarterly	1	8	(529, 76, 151)
	M3-Monthly	1	18	(999, 144, 285)
Anomaly detection (TSB-UAD)	MITDB	1		
	ECCG	1		
	MGAB	1	-	(50%, -, 50%)
	SVDB	1		

Forecasting: (1) *Linear Probing*: The model is linear-probed (MOMENT_{LP}) by freezing all parameters except for those in the reconstruction or forecasting head. (2) *LoRA Fine-tuning*: Based on linear probing, LoRA modules are added to all linear layers for fine-tuning. (3) *Reconstructed Forecasting Head*: The forecasting head is reconstructed using the four methods in sec 4.3: *Proj Down*, *Avg Pool*, *Less Feature* and *Conv 2D*. (4) *AdaLoRA*: *ProjDown* forecasting head with AdaLoRA method. (5) *TRACE*: In addition to the reconstructed forecasting head, the Gated DISC method is incorporated. The main model for TRACE uses the *Proj Down* method for dimensionality reduction in the forecasting head.

Anomaly Detection: (1) *Linear Probing*: The model is linear-probed (MOMENT_{LP}) by freezing all parameters except for those in the reconstruction or forecasting head. (2) *LoRA Fine-tuning*: Based on linear probing, LoRA modules are added to all linear layers for fine-tuning. (3) *TRACE*: The DISC-LoRA method is applied on top of Linear Probing for anomaly detection.

5.3. Settings

5.3.1. model hyper-parameters

The hyperparameters used for training our models are shown in the Table 3:

Table 3: Main experiment parameter settings of the TRACE method

Model	Hyper-parameters	Value
MOMENT(TRACE)	dimension of model	768
	number of layers	12
	number of heads	12
	Sequence length	512
	patch length	8
	dimension of feedforward layer	3072
	lora rank γ	2
	max rank of AdaLoRA	4
	total mask percentage	95%
	mask percentage by step	10%
	forecast horizon	{192,336,720}
Dimensionality Reduction Factor β	8	

5.3.2. training hyper-parameters

For the long-term forecasting task, during the model training phase, we use a backtracking window of length $L = 512$ for training all models. We predict the Exchange dataset with $T = 96$ and $T = 192$ time steps, while for the other datasets, the prediction horizons are set to $T = 192$ and $T = 720$ time steps. We evaluate the models using Mean Squared Error (MSE) and Mean Absolute Error (MAE) as metrics.

The initial learning rate during training is set to 2×10^{-4} , with a maximum of 15 epochs for training. The validation and test sets are split according to the rules outlined in Table 2, and we adopt the OneCycleLR strategy for early stopping. The batch size used during model training is 16.

For the short-term forecasting task, we follow the settings defined in MOMENT. For the Monthly dataset, the prediction horizon $T = 18$; for the Quarterly dataset, $T = 8$; and for the Yearly dataset, $T = 6$.

For the anomaly detection task, the training parameters remain consistent with those used in the forecasting tasks.

5.4. Main Experimental Results

5.4.1. Long-horizon Forecasting

Table 4: Long-term forecasting performance measured using Mean Squared Error (MSE) and Mean Absolute Error (MAE). Results are averaged over five random experiments. Bold and underlined values indicate the best and second-best results, respectively.

Forecasting Horizon	MOMENT _{LP}		MOMENT _{LP+LoRA}		MOMENT _{Proj down}		MOMENT _{AdaLoRA}		TRACE		
	MSE	MAE	MSE	MAE	MSE	MAE	MSE	MAE	MSE	MAE	
ETTh1	192	0.417	0.430	0.420	0.433	0.415	0.430	<u>0.414</u>	<u>0.429</u>	0.412	0.427
	336	0.432	0.449	0.435	0.450	<u>0.429</u>	<u>0.446</u>	0.430	<u>0.446</u>	0.428	0.444
	720	0.476	0.487	0.479	0.490	0.475	0.486	<u>0.472</u>	<u>0.484</u>	0.470	0.481
ETTh2	192	0.347	0.389	0.348	0.388	0.347	0.386	0.345	0.384	<u>0.346</u>	<u>0.385</u>
	336	0.374	0.413	0.376	0.417	<u>0.373</u>	<u>0.412</u>	0.376	0.416	0.370	0.409
	720	0.397	0.436	0.398	0.437	<u>0.396</u>	<u>0.435</u>	0.399	0.437	0.395	0.434
ETTm1	192	0.328	0.368	0.329	0.371	<u>0.327</u>	<u>0.367</u>	0.330	0.372	0.326	0.366
	336	0.355	0.388	0.356	0.389	0.353	0.387	<u>0.352</u>	<u>0.386</u>	0.351	0.384
	720	0.408	0.419	0.411	0.422	<u>0.406</u>	<u>0.417</u>	0.407	0.418	0.405	0.416
ETTm2	192	0.228	0.299	0.229	0.300	0.226	0.297	<u>0.227</u>	<u>0.298</u>	0.228	0.299
	336	0.276	0.329	0.279	0.331	0.276	0.328	<u>0.275</u>	<u>0.327</u>	0.274	0.325
	720	0.360	0.386	0.362	0.387	<u>0.360</u>	<u>0.384</u>	0.363	0.388	0.359	0.383
Weather	192	0.204	0.254	0.207	0.258	<u>0.203</u>	<u>0.252</u>	0.206	0.257	0.200	0.248
	336	0.253	0.294	0.255	0.296	<u>0.252</u>	<u>0.293</u>	0.254	0.296	0.251	0.292
	720	0.323	0.340	0.324	0.340	0.321	0.339	<u>0.318</u>	<u>0.338</u>	0.317	0.337
Exchange	96	0.122	0.249	0.119	0.247	0.105	0.230	0.111	0.237	<u>0.108</u>	<u>0.233</u>
	192	0.225	0.342	0.222	0.340	0.214	0.333	<u>0.210</u>	<u>0.329</u>	0.206	0.326
	336	0.317	0.434	0.320	0.437	<u>0.315</u>	<u>0.433</u>	0.316	0.434	0.313	0.430
ECL	192	0.158	0.254	0.160	0.255	0.153	0.248	0.149	0.244	<u>0.151</u>	<u>0.246</u>
	336	<u>0.169</u>	<u>0.266</u>	0.172	0.268	0.170	0.267	0.171	0.267	0.167	0.264
	720	0.210	0.301	<u>0.209</u>	<u>0.300</u>	0.208	0.298	0.210	0.301	0.208	0.298

Table 4 presents the main experimental results for long-term forecasting, comparing the performance of the MOMENT model under five conditions: linear probing, full LoRA fine-tuning, reconstruction of the forecasting head (projection down, with $\beta = 8$), AdaLoRA (with projection down head) and TRACE (Gated DSIC and projection down with $\beta = 8$) fine-tuning. The results are evaluated in terms of MSE and MAE across different prediction lengths.

By comparing the results, we observe that the reconstructed forecasting head: MOMENT_{Proj down}, achieves lower MSE and MAE across all long-term forecasting tasks compared to linear probing (MOMENT_{LP}) and full LoRA fine-tuning (MOMENT_{LP+LoRA}). Our proposed **TRACE** outperforms other approaches, including AdaLoRA, on the majority of datasets.

Static Test: To evaluate the performance of our proposed TRACE model against the state-of-the-art MOMENT_{LP}, we conducted a statistical analysis using the dataset’s actual values and the predictions from both

models. Our objective was to assess the accuracy and reliability of these models under various conditions.

To quantify predictive performance, we employed a binary classification framework. A prediction was considered accurate if the absolute error between the predicted and actual values was below a predetermined threshold of 5.0[27]; otherwise, it was deemed inaccurate.

We constructed a 2×2 contingency table to systematically categorize the predictive outcomes of both models. The confusion matrix for the classification results is as follows:

$$\begin{bmatrix} 158993571 & 1108 \\ 985 & 4932 \end{bmatrix}.$$

The four categories were defined as: both models correctly predicted (158993571 instances), TRACE correctly predicted while MOMENT_{LP} incorrectly predicted (1108 instances), TRACE incorrectly predicted while MOMENT_{LP} correctly predicted (985 instances), and both models incorrectly predicted (4932 instances). This classification enabled a detailed comparative analysis of the models' performance.

To statistically validate the observed differences in misclassification rates, we applied the McNemar test. This non-parametric test is particularly suitable for paired nominal data, such as the binary outcomes observed in this study. The McNemar test statistic is computed as: $\chi^2 = \frac{(b-c)^2}{b+c}$, where b represents the number of cases where TRACE incorrectly predicted while MOMENT_{LP} correctly predicted, and c represents the number of cases where TRACE correctly predicted while MOMENT_{LP} incorrectly predicted.

The test results yielded a McNemar statistic of 7.23 with an associated p-value of 0.0071. Given the conventional alpha level of 0.05, the p-value indicates a statistically significant difference in the proportion of misclassifications between the two models. Specifically, the results suggest that TRACE consistently produced more correct predictions in cases where MOMENT_{LP} failed, indicating that TRACE may offer superior performance in certain scenarios.

Computational Cost: Table 5 presents the computational costs of different models on the Electricity dataset, along with experimental results under a prediction horizon of 720 and $\beta=4$. The reported results represent the average of five independent runs.

Table 5: Computational cost on Electricity dataset.

	Models	Parameters(M)	Training time(s)	Inference time (s)
Forecasting Head	linear probing	35.38	387.32	41.70
	Proj Down	8.99	251.34	27.45
	Avg Pool	8.99	223.56	26.34
	Less Feature	8.47	219.95	27.12
	Conv2D	8.84	260.17	33.43
Backbone	full LoRA	4.75	729.58	38.36
	AdaLoRA	3.43	643.31	37.95
	TRACE	2.89	942.86	38.17

5.4.2. Short-horizon Forecasting

Table 6: Zero-shot short-horizon forecasting performance on a subset of the M3 and M4 datasets measured using sMAPE.

Datasets		MOMENT _{LP}		MOMENT _{LP+LoRA}		MOMENT _{Proj down}		TRACE	
		M4	FR	M4	FR	M4	FR	M4	FR
M3	Yearly	17.03	17.13	17.21	17.37	17.01	17.85	16.88	17.49
	Quarterly	10.47	10.73	10.81	11.36	10.34	10.74	10.25	10.70
	Monthly	16.35	17.11	16.49	17.26	16.32	17.10	16.28	17.03
M4	Yearly	-	15.11	-	15.37	-	14.98	-	14.83
	Quarterly	-	12.86	-	13.14	-	12.55	-	12.03
	Monthly	-	16.26	-	16.73	-	15.98	-	15.87

For short-horizon forecasting, we adopt the zero-shot setting proposed by Oreshkin [28]. Specifically, we first fine-tune MOMENT on a **source dataset** with a forecasting head and then assess its performance on a **target dataset** without any additional fine-tuning. It is consistent with the setup in MOMENT [23].

We evaluated our model’s zero-forecasting performance on the M3 and M4 datasets. We maintained the same settings as in the MOMENT[23], following the dataset splits for training, testing, and forecasting horizons as defined in the M3 and M4 competitions. The evaluation metric used was sMAPE ([29]; [30]). Due to the scarcity of daily, hourly, and weekly frequency data, it is challenging for deep models to fully leverage their zero-shot capabilities in these cases. Table 7 presents the correspondence between source and target datasets. The setup for the Fred dataset follows [23] and [28].

Table 6 show that, under the sMAPE evaluation metric, the reconstructed forecasting head (MOMENT_{Proj down}) and the TRACE method both outper-

Table 7: Experimental settings for short-horizon forecasting experiments for varying source and target datasets.

Source Dataset→ Target↓	M4	Fred
M4		
Yearly	-	Yearly
Quarterly	-	Yearly
Monthly	-	Monthly
M3		
Yearly	Yearly	Yearly
Quarterly	Quarterly	Quarterly
Monthly	Monthly	Monthly

form linear probing and full fine-tuning.

5.4.3. Anomaly Detection

Table 8: Anomaly detection performance on selected datasets from the UCR Anomaly Archive

Adj-F1	MITDB	ECG			MGAB			SVDB	
Index	100	801	803	1406	2	3	4	842	859
MOMENT _{LP}	0.819	0.695	0.968	0.761	0.429	0.437	0.459	0.828	0.864
TRACE	0.820	0.702	0.969	0.761	0.444	0.448	0.460	0.828	0.865

In the anomaly detection task, we selected subsets of datasets from MITDB, ECG, MGAB, and SVDB. Since the task of anomaly detection involves a relatively small number of parameters in the prediction head, which is not suitable for dimensionality reduction or reconstruction, in this context, TRACE is equivalent to Gated DSIC. Table 8 show that TRACE generally outperforms the linear probing.

5.4.4. Natural Language Processing Task

While our work focuses on continuous temporal data, evaluating on natural language tasks is necessary to assess the method’s applicability across sequential modalities. As natural language represents discrete sequences, such comparison reveals the adaptability and robustness of our approach beyond traditional time series, offering valuable insights into its generalization across both low- and high-frequency domains. These findings can serve as a reference and inspiration for future research exploring the intersection of temporal modeling and discrete sequence processing.

Table 9: Overall comparison on the GLUE benchmark with the DeBERTaV3-base backbone. Results are averaged over five random experiments. Bold and underlined values indicate the best and second-best results, respectively. The initial LoRA rank is set to 4 and then halved according to our method.

Method	Trainable Params	Avg. Score	MNLI	QQP	QNLI	SST-2	CoLA	STS-B	MRPC	RTE
Full Fine-tuning	184M	88.62	90.01	91.10	94.03	95.63	69.19	91.60	89.46	86.94
Adapter	0.35M	87.57	90.28	89.41	93.52	94.38	67.80	91.08	89.75	84.36
LoRA	0.33M	88.12	90.34	90.26	93.87	94.84	68.71	91.63	89.71	85.56
AdaLoRA	0.35M	88.93	90.18	90.37	<u>94.29</u>	95.62	70.04	91.57	<u>90.34</u>	87.06
MOELoRA	0.92M	88.89	90.26	90.31	94.08	95.53	70.47	91.52	90.26	<u>87.64</u>
DoRA	0.33M	<u>89.00</u>	<u>90.43</u>	90.16	94.17	<u>95.80</u>	70.26	<u>91.68</u>	90.12	87.38
Proposed Method										
Our Method	0.33M	89.51	90.76	<u>90.66</u>	94.72	96.17	71.95	92.33	90.86	88.63

Table 10: Comparison of different PEFT methods for two backbone models (Qwen2.5 0.5B). Results are presented as accuracy for each task and averaged across five random experiments. The LLM used is the Qwen2.5 0.5B model, with the LoRA rank initially set to 32 and then halved.

Method (Million)	Trainable Params (acc)	BoolQ (acc)	ARC-e (acc)	ARC-c (acc)
Baseline(Qwen2.5 0.5B)				
Adapter	9.0M	78.36	71.04	53.26
LoRA	8.8M	78.94	72.78	54.38
AdaLoRA	8.9M	80.32	73.96	54.23
Our Method	8.8M	82.49	74.67	55.64

We are currently conducting experiments on English datasets in the field of natural language processing. The datasets are sourced from the GLUE benchmark: paraphrase detection (MRPC, QQP), sentiment classification (SST-2), natural language inference (MNLI, RTE, QNLI), and linguistic acceptability (CoLA). We also consider three challenging QA datasets to evaluate the performance of our method on large language models: three common-sense question-answering benchmark tasks—ARC-e, ARC-c [31], and BoolQ [32].

Experimental results on the GLUE benchmark are shown in Table 9, and those on the QA datasets are presented in Table 10. Our method, Gated-DISC, achieves the best or second-best performance with the smallest number of trainable parameters in both settings.

5.5. Ablation studies and further analysis

In this section, we analyze the effects of dimensionality reduction factor β , forecasting head reconstruction methods, and LoRA rank on model performance. Results indicate that excessively large β degrades accuracy, with optimal values typically being 4 or 8. For long-horizon forecasting, reconstruction method performance varies by task. Additionally, LoRA rank should remain moderate to avoid overfitting, as the pre-trained time-series backbone requires only minimal fine-tuning on the target dataset. Ablation studies confirm TRACE’s strong stability.

5.5.1. Impact of the Dimensionality Reduction Factor β

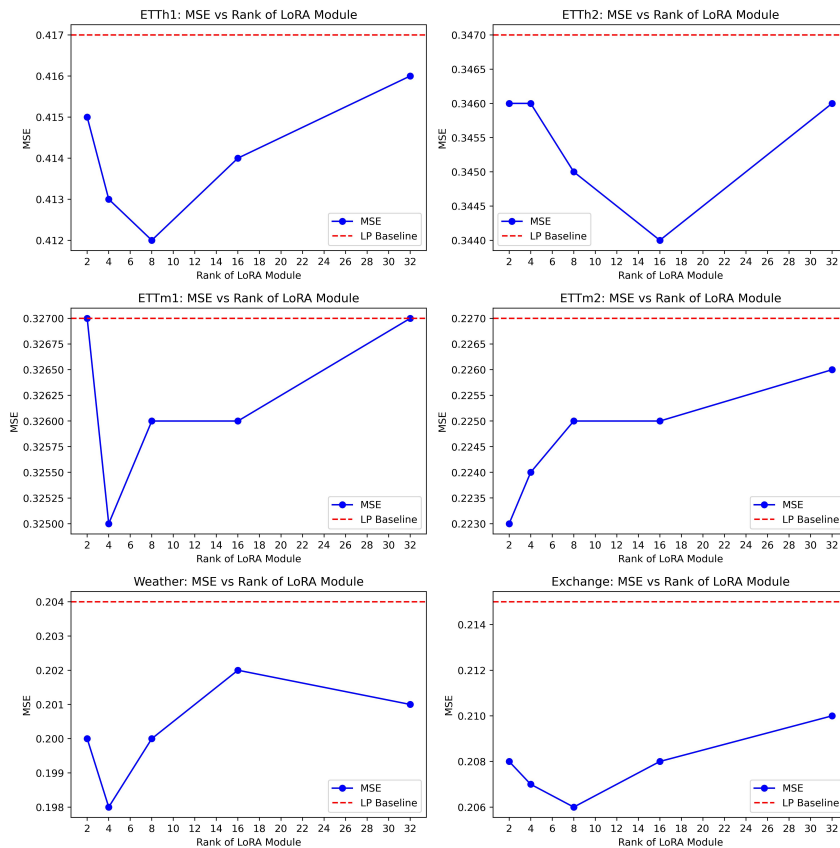


Figure 2: MSE Comparison between TRACE Method and Linear Probing on Different Datasets at Different β (Prediction Horizon: 192, Forecasting Head: Projection Down)

Figure 2 illustrates the effect of varying the dimensionality reduction factor on MSE under the TRACE method, with a forecast horizon of 192 and the Projection Down reconstruction for different tasks. The analysis shows that the overall fluctuation is minimal, with the maximum fluctuation in a single task not exceeding 1%. The optimal dimensionality reduction factor, β , typically takes values of 4 or 8. A larger value of β reduces the number of trainable parameters in the prediction head, which in turn negatively impacts the model’s forecasting performance. Figure 3 presents the results for a forecast horizon of 720, where similar conclusions can be drawn.

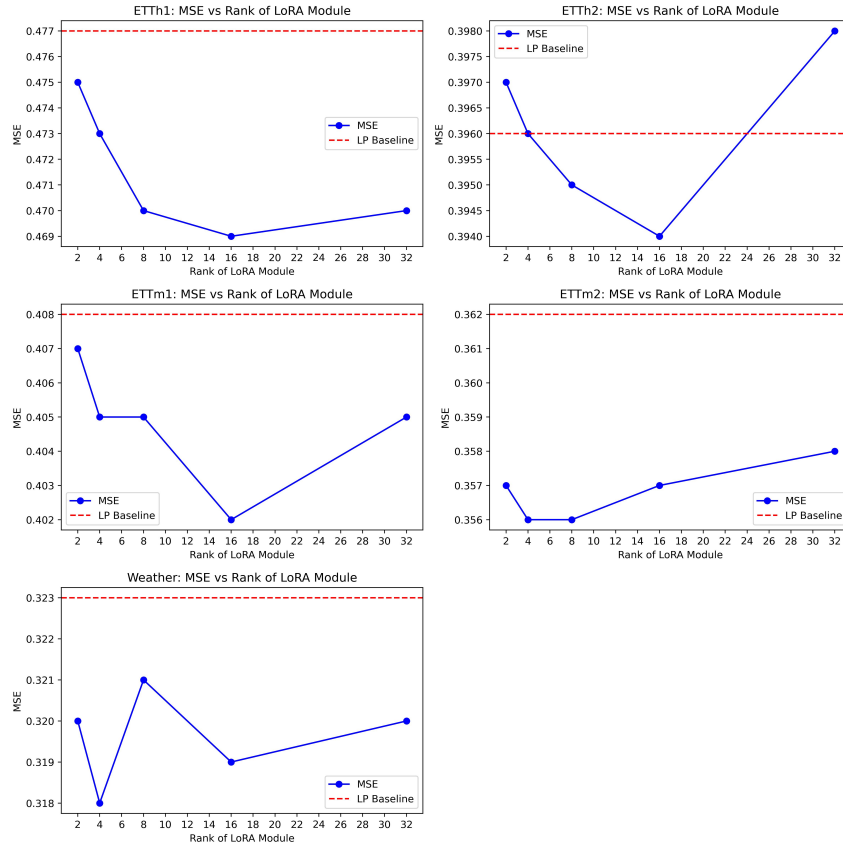


Figure 3: MSE Comparison between TRACE Method and Linear Probing on Different Datasets at Different β (Prediction Horizon: 720, Forecasting Head: Projection Down)

5.5.2. Impact of Different Prediction Heads

Table 11: Long-term forecasting performance measured using Mean Squared Error (MSE) and Mean Absolute Error (MAE) in different reconstruction forecasting head. Bold values indicate the best.

Forecasting Horizon	MOMENT _{LP}		TRACE _{Less Feature}		TRACE _{Avg Pool}		TRACE _{Conv2D}		TRACE _{Proj Down}		
	MSE	MAE	MSE	MAE	MSE	MAE	MSE	MAE	MSE	MAE	
ETTh1	192	0.417	0.430	0.413	0.428	0.414	0.429	0.423	0.435	0.412	0.427
	336	0.432	0.449	0.428	0.445	0.427	0.443	0.437	0.455	0.428	0.444
	720	0.476	0.487	0.469	0.480	0.471	0.482	0.479	0.491	0.470	0.481
ETTh2	192	0.347	0.389	0.347	0.388	0.345	0.386	0.353	0.394	0.345	0.385
	336	0.374	0.413	0.369	0.407	0.368	0.407	0.377	0.417	0.370	0.409
	720	0.396	0.435	0.395	0.434	0.396	0.435	0.416	0.457	0.395	0.434
ETTm1	192	0.327	0.368	0.326	0.367	0.325	0.365	0.333	0.375	0.326	0.366
	336	0.355	0.388	0.351	0.385	0.352	0.386	0.354	0.388	0.351	0.384
	720	0.408	0.419	0.403	0.414	0.404	0.415	0.417	0.428	0.405	0.416
ETTm2	192	0.227	0.299	0.228	0.300	0.226	0.298	0.231	0.305	0.228	0.299
	336	0.276	0.329	0.276	0.328	0.273	0.325	0.287	0.339	0.274	0.325
	720	0.360	0.386	0.358	0.384	0.354	0.380	0.373	0.401	0.359	0.383
Weather	192	0.204	0.254	0.201	0.248	0.200	0.248	0.211	0.260	0.200	0.248
	336	0.253	0.294	0.250	0.291	0.251	0.293	0.267	0.308	0.251	0.292
	720	0.323	0.340	0.319	0.339	0.317	0.336	0.328	0.345	0.317	0.337
Exchange	96	0.122	0.249	0.103	0.228	0.105	0.229	0.119	0.245	0.108	0.233
	192	0.225	0.342	0.211	0.330	0.208	0.327	0.228	0.345	0.206	0.326
	336	0.317	0.434	0.314	0.432	0.312	0.430	0.329	0.347	0.313	0.430

Under the condition of the same dimensionality reduction factor ($\beta = 8$), we compared the performance of the TRACE method with different reconstruction approaches for the forecasting head and the original linear probing method on long-term forecasting datasets. Specifically, TRACE_{Proj Down}, TRACE_{Less Feature}, TRACE_{Avg Pool}, and TRACE_{Conv2D} refer to the different forecasting head reconstruction methods previously introduced.

The comparison results in Table 11, in nearly all tasks, the TRACE method outperforms Linear Probing or performs equivalently. However, when reconstructing the prediction head with Conv2D, the performance is generally suboptimal, and in most cases, it is inferior to Linear Probing, with a performance gap of within 3.8%. A possible reason for this is that 2D convolution may not be well-suited for extracting features from time series with independent channels, as fluctuations between covariates can introduce interference.

However, the performance of different reconstruction methods varies across tasks, with no single method being consistently optimal for all tasks. This suggests that, in practical applications, it may be beneficial to tailor the

forecasting head to suit the specific task at hand.

5.5.3. Impact of LoRA Rank

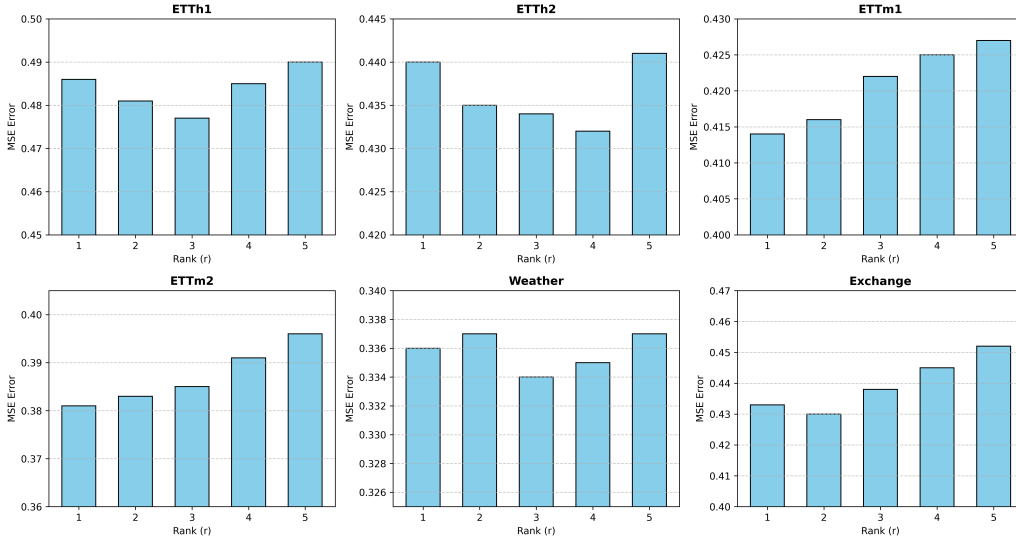


Figure 4: The impact of the rank size of the incremental matrix on model performance measured using Mean Squared Error (MSE)

Figure 4 illustrates the performance variations of the TRACE method on different long-term forecasting datasets when only the LoRA rank γ is changed, while keeping all other parameters consistent with the main experiment settings. The analysis indicates that the optimal rank value falls within the range of 2 to 3. This ablation study also confirms that when fine-tuning time series foundation models with LoRA, selecting an excessively large rank γ is not advisable.

5.5.4. Case Analysis

We conducted a case analysis on four ETT datasets (ETTh1, ETTh2, ETTm1, and ETTm2) by plotting the ground truth time series of the test set along with the predicted sequences from MOMENT_{LP} , $\text{MOMENT}_{Proj\ down}$, and $\text{TRACE}_{Proj\ Down}$, as illustrated in Figure 5. In the figure, the predictions generated by the TRACE method are represented by the yellow curve, which more closely aligns with the green curve denoting the ground truth compared to the results from other models.

To provide a more intuitive comparison, we visualize partial forecasts on the ETTh2 test set. For a prediction horizon of 192 (Figure 6, TRACE in Figure 6f), our method shows better alignment with the true values, especially during volatile periods (e.g., steps 460–500). With a horizon of 720 (Figure 7), TRACE in Figure 7f captures the drop trend around step 500 more accurately than competing methods.

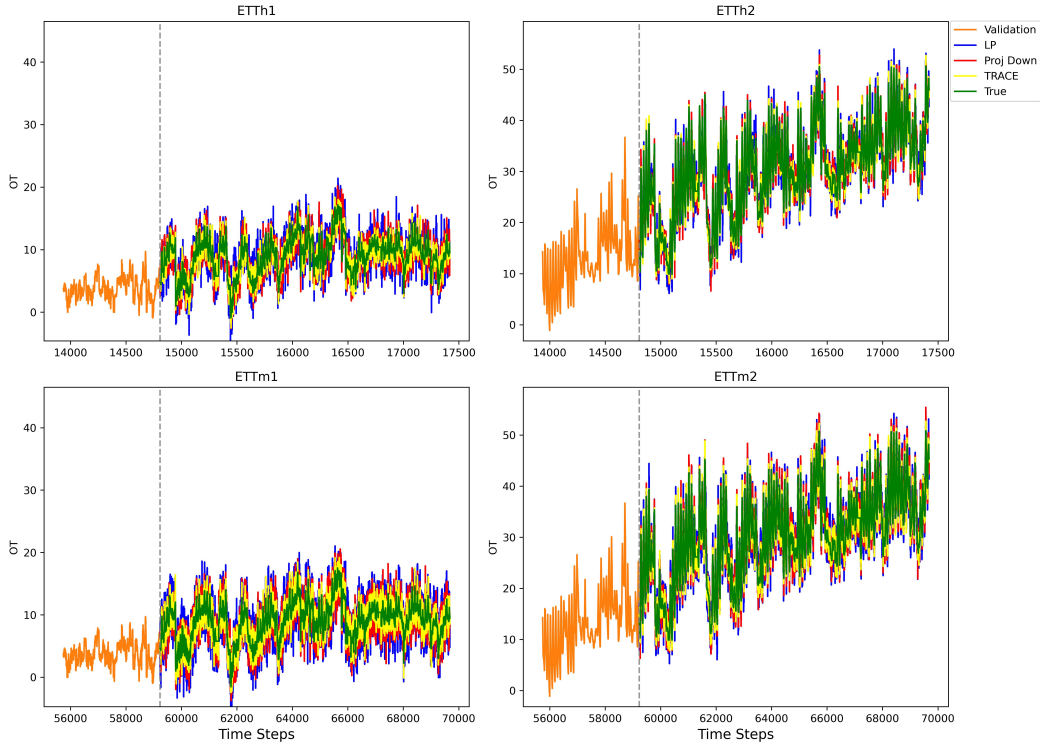


Figure 5: Comparison of true values on the ETT long-horizon forecasting dataset’s test set with predicted values from different models

5.6. Conclusions and future work

This paper proposes an efficient fine-tuning method for time-series foundation models, TRACE: Time Series Parameter Efficient Fine-tuning. It leverages the Gated DSIC method to perform unbiased selection of LoRA modules based on their importance and sensitivity, filtering out unimportant LoRA modules while retaining those that are truly effective in fine-tuning.

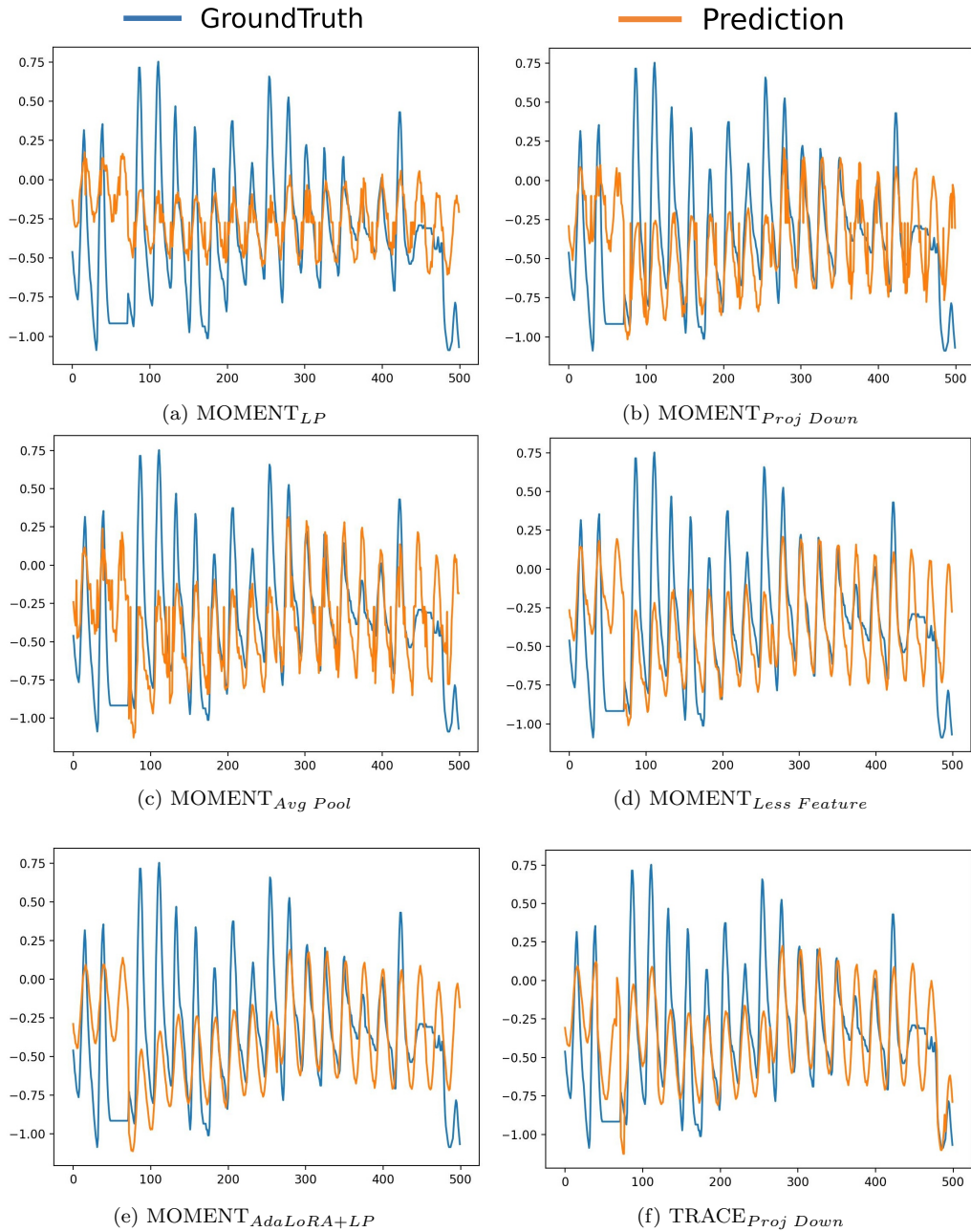


Figure 6: Forecasting cases using the input-512-predict-192 configuration.

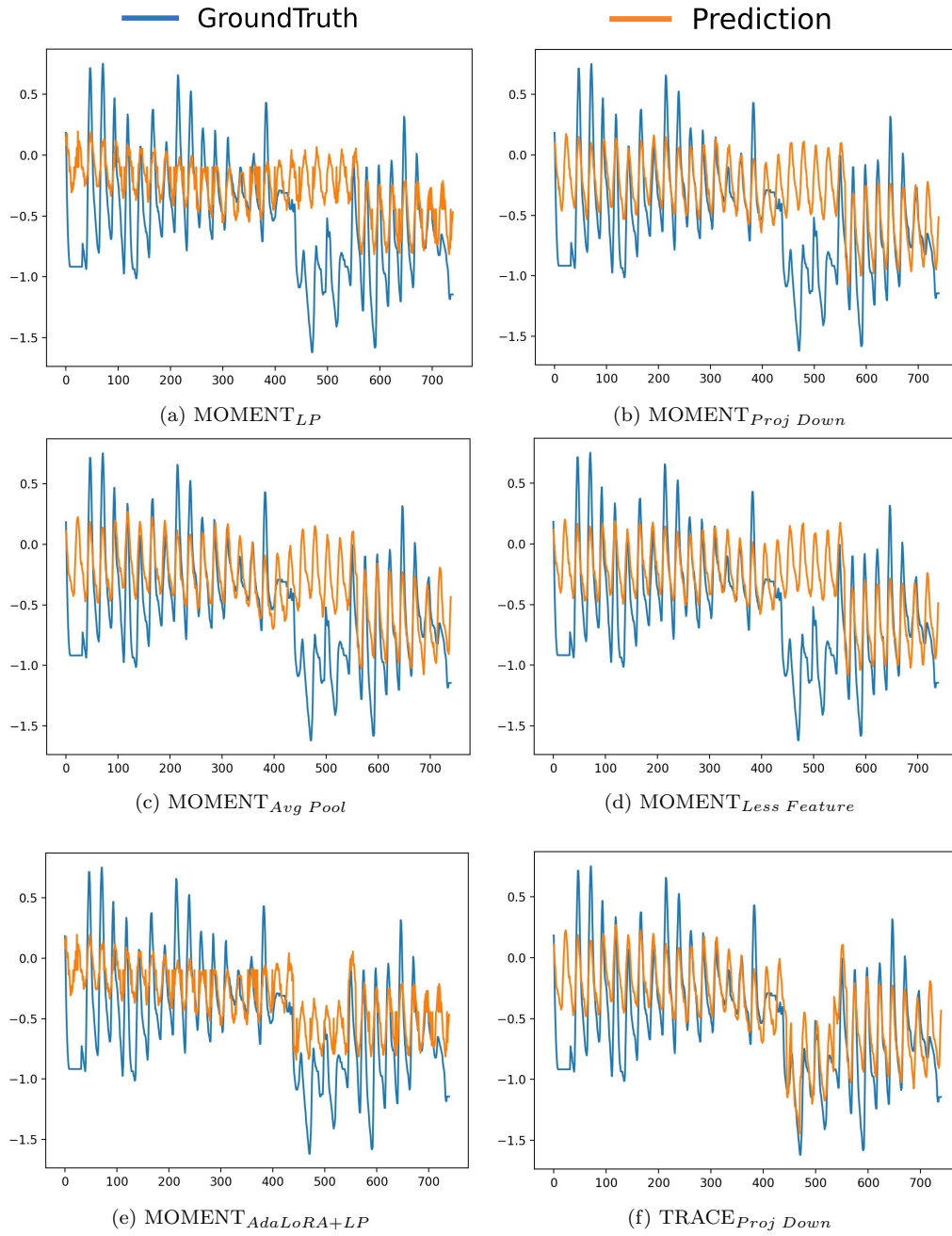


Figure 7: Forecasting cases using the input-512-predict-720 configuration.

TRACE demonstrates superior performance in long-term forecasting, short-term forecasting, and anomaly detection tasks.

In long-term forecasting, the prediction head often contains an excessive number of parameters, making it prone to overfitting during fine-tuning and limiting the generalization ability of the foundation model. To address this, we propose various approaches for reconstructing the prediction head, which outperform linear probing in our experiments.

A potential limitation of our approach is that the retained LoRA modules (in terms of proportion and rank) may vary across different downstream tasks and forecasting horizons. One possible solution is to store the trained incremental matrix parameters under different conditions, enabling a plug-and-play mechanism across scenarios. Furthermore, our experiments reveal substantial variability in fine-tuning performance across different tasks and datasets. Exploring the deployment of time-series foundation models in real-world time-series applications and investigating their potential in multimodal learning could be promising directions for future research.

References

- [1] R. J. Hyndman, A. B. Koehler, R. D. Snyder, S. Grose, A state space framework for automatic forecasting using exponential smoothing methods, *International Journal of forecasting* 18 (3) (2002) 439–454.
- [2] A. A. Ariyo, A. O. Adewumi, C. K. Ayo, Stock price prediction using the arima model, in: *2014 UKSim-AMSS 16th international conference on computer modelling and simulation*, IEEE, 2014, pp. 106–112.
- [3] S. Hochreiter, J. Schmidhuber, Long short-term memory, *Neural computation* 9 (8) (1997) 1735–1780.
- [4] J. Chung, C. Gulcehre, K. Cho, Y. Bengio, Empirical evaluation of gated recurrent neural networks on sequence modeling, *arXiv preprint arXiv:1412.3555* (2014).
- [5] J. H. Stock, M. W. Watson, Vector autoregressions, *Journal of Economic perspectives* 15 (4) (2001) 101–115.
- [6] T. Chen, C. Guestrin, Xgboost: A scalable tree boosting system, in: *Proceedings of the 22nd acm sigkdd international conference on knowledge discovery and data mining*, 2016, pp. 785–794.
- [7] G. Ke, Q. Meng, T. Finley, T. Wang, W. Chen, W. Ma, Q. Ye, T.-Y. Liu, Lightgbm: A highly efficient gradient boosting decision tree, *Advances in neural information processing systems* 30 (2017).
- [8] C. Lea, M. D. Flynn, R. Vidal, A. Reiter, G. D. Hager, Temporal convolutional networks for action segmentation and detection, in: *proceedings of the IEEE Conference on Computer Vision and Pattern Recognition*, 2017, pp. 156–165.
- [9] A. Vaswani, N. Shazeer, N. Parmar, J. Uszkoreit, L. Jones, A. N. Gomez, Ł. Kaiser, I. Polosukhin, Attention is all you need, *Advances in neural information processing systems* 30 (2017).
- [10] H. Zhou, S. Zhang, J. Peng, S. Zhang, J. Li, H. Xiong, W. Zhang, Informer: Beyond efficient transformer for long sequence time-series forecasting, in: *Proceedings of the AAAI conference on artificial intelligence*, Vol. 35, 2021, pp. 11106–11115.

- [11] Y. Liu, T. Hu, H. Zhang, H. Wu, S. Wang, L. Ma, M. Long, itransformer: Inverted transformers are effective for time series forecasting, arXiv preprint arXiv:2310.06625 (2023).
- [12] T. Zhou, Z. Ma, Q. Wen, X. Wang, L. Sun, R. Jin, Fedformer: Frequency enhanced decomposed transformer for long-term series forecasting, in: International conference on machine learning, PMLR, 2022, pp. 27268–27286.
- [13] Y. Nie, N. H. Nguyen, P. Sinthong, J. Kalagnanam, A time series is worth 64 words: Long-term forecasting with transformers, arXiv preprint arXiv:2211.14730 (2022).
- [14] A. Garza, C. Challu, M. Mergenthaler-Canseco, Timegpt-1, arXiv preprint arXiv:2310.03589 (2023).
- [15] D. Cao, F. Jia, S. O. Arik, T. Pfister, Y. Zheng, W. Ye, Y. Liu, Tempo: Prompt-based generative pre-trained transformer for time series forecasting, arXiv preprint arXiv:2310.04948 (2023).
- [16] A. Das, W. Kong, R. Sen, Y. Zhou, A decoder-only foundation model for time-series forecasting, in: Forty-first International Conference on Machine Learning, 2024.
- [17] G. Woo, C. Liu, A. Kumar, C. Xiong, S. Savarese, D. Sahoo, Unified training of universal time series forecasting transformers (2024).
- [18] S. Gao, T. Koker, O. Queen, T. Hartvigsen, T. Tsiligkaridis, M. Zitnik, Units: Building a unified time series model, arXiv e-prints (2024) arXiv:2403.
- [19] C. Sun, H. Li, Y. Li, S. Hong, Test: Text prototype aligned embedding to activate llm’s ability for time series, arXiv preprint arXiv:2308.08241 (2023).
- [20] M. Jin, S. Wang, L. Ma, Z. Chu, J. Y. Zhang, X. Shi, P.-Y. Chen, Y. Liang, Y.-F. Li, S. Pan, et al., Time-llm: Time series forecasting by reprogramming large language models, arXiv preprint arXiv:2310.01728 (2023).

- [21] K. Rasul, A. Ashok, A. R. Williams, A. Khorasani, G. Adamopoulos, R. Bhagwatkar, M. Biloš, H. Ghonia, N. Hassen, A. Schneider, et al., Lag-llama: Towards foundation models for time series forecasting, in: R0-FoMo: Robustness of Few-shot and Zero-shot Learning in Large Foundation Models, 2023.
- [22] N. Shazeer, Glu variants improve transformer, arXiv preprint arXiv:2002.05202 (2020).
- [23] M. Goswami, K. Szafer, A. Choudhry, Y. Cai, S. Li, A. Dubrawski, Moment: A family of open time-series foundation models, arXiv preprint arXiv:2402.03885 (2024).
- [24] H. Zhou, S. Zhang, J. Peng, S. Zhang, J. Li, H. Xiong, W. Zhang, Informer: Beyond efficient transformer for long sequence time-series forecasting, in: The Thirty-Fifth AAAI Conference on Artificial Intelligence, AAAI 2021, Virtual Conference, Vol. 35, AAAI Press, 2021, pp. 11106–11115.
- [25] R. Godahewa, C. Bergmeir, G. I. Webb, R. J. Hyndman, P. Montero-Manso, Monash time series forecasting archive, arXiv preprint arXiv:2105.06643 (2021).
- [26] J. Paparrizos, Y. Kang, P. Boniol, R. S. Tsay, T. Palpanas, M. J. Franklin, Tsb-uad: an end-to-end benchmark suite for univariate time-series anomaly detection, Proceedings of the VLDB Endowment 15 (8) (2022) 1697–1711.
- [27] H. Jiang, D. Liu, X. Ding, Y. Chen, H. Li, Tcm: An efficient lightweight mlp-based network with affine transformation for long-term time series forecasting, Neurocomputing 617 (2025) 128960.
- [28] B. N. Oreshkin, D. Carпов, N. Chapados, Y. Bengio, Meta-learning framework with applications to zero-shot time-series forecasting, in: Proceedings of the AAAI conference on artificial intelligence, Vol. 35, 2021, pp. 9242–9250.
- [29] B. N. Oreshkin, D. Carпов, N. Chapados, Y. Bengio, N-beats: Neural basis expansion analysis for interpretable time series forecasting, arXiv preprint arXiv:1905.10437 (2019).

- [30] H. Wu, T. Hu, Y. Liu, H. Zhou, J. Wang, M. Long, Timesnet: Temporal 2d-variation modeling for general time series analysis, arXiv preprint arXiv:2210.02186 (2022).
- [31] P. Clark, I. Cowhey, O. Etzioni, T. Khot, A. Sabharwal, C. Schoenick, O. Tafjord, Think you have solved question answering? try arc, the ai2 reasoning challenge, arXiv preprint arXiv:1803.05457 (2018).
- [32] C. Clark, K. Lee, M.-W. Chang, T. Kwiatkowski, M. Collins, K. Toutanova, Boolq: Exploring the surprising difficulty of natural yes/no questions, arXiv preprint arXiv:1905.10044 (2019).

Appendix A. Multiple Variants of Reconstructed Prediction Heads and Their Parameter Complexity

Proj Down: A factorized linear architecture reduces dimensions via two projections. For input $\mathbf{X} \in \mathbb{R}^{B \times N \times D}$ (B : batch size, N : patches, D : embedding dimension), a learnable projection $\mathbf{W}_1 \in \mathbb{R}^{D \times D/\beta}$ reduces D by factor β , yielding $\mathbf{X}' = \mathbf{X}\mathbf{W}_1$. Flattened features $\text{Flatten}(\mathbf{X}') \in \mathbb{R}^{B \times (N \cdot D/\beta)}$ are projected via $\mathbf{W}_2 \in \mathbb{R}^{(N \cdot D/\beta) \times H}$ to produce horizon predictions $\hat{\mathbf{Y}} \in \mathbb{R}^{B \times H}$. This reduces parameters from $\mathcal{O}(NDH)$ to $\mathcal{O}(D^2/\beta + NDH/\beta)$.

Less Feature: Non-learnable truncation retains only the first D/β dimensions along the feature axis: $\mathbf{X}' = \mathbf{X}_{:, :, :D/\beta}$. Flattened features $\text{Flatten}(\mathbf{X}') \in \mathbb{R}^{B \times (N \cdot D/\beta)}$ are mapped to horizon H via $\mathbf{W} \in \mathbb{R}^{(N \cdot D/\beta) \times H}$. Parameter complexity is $\mathcal{O}(NDH/\beta)$, trading simplicity for potential information loss.

Avg Pool: Spatial pooling combines 2D average pooling and learnable projection. Input $\mathbf{X} \in \mathbb{R}^{B \times C \times N \times D}$ (C : channels) is spatially downsampled via AvgPool2d:

$$\mathbf{X}' = \text{AvgPool2d}(\mathbf{X}), \quad \mathbf{X}' \in \mathbb{R}^{B \times C \times N/2 \times D}. \quad (\text{A.1})$$

A linear layer $\mathbf{W}_1 \in \mathbb{R}^{D \times D/\beta}$ compresses features, and flattened features $\text{Flatten}(\mathbf{X}'') \in \mathbb{R}^{B \times (C \cdot N/2 \cdot D/\beta)}$ are mapped to horizon H via \mathbf{W}_2 . This balances locality preservation and efficiency.

Conv 2D: Temporal convolution employs strided depthwise 1D convolutions for subsampling. For input $\mathbf{X} \in \mathbb{R}^{B \times C \times N \times D}$, a kernel $\mathbf{K} \in \mathbb{R}^{1 \times k}$ with stride $s = \beta$ operates along the temporal axis:

$$\mathbf{X}' = \text{Conv2d}(\mathbf{X}), \quad \mathbf{X}' \in \mathbb{R}^{B \times C \times \lfloor N/s \rfloor \times D}. \quad (\text{A.2})$$

Convolution reduces sequence length by β , followed by a linear layer $\mathbf{W} \in \mathbb{R}^{(C \cdot \lfloor N/s \rfloor \cdot D) \times H}$. Parameter cost is $\mathcal{O}(k)$ for convolution and $\mathcal{O}(NDH/\beta)$ for projection.

Appendix B. Computational Resources

Hardware :

- GPU: NVIDIA V100 (32GB memory) \times 2
- CPU: Xeon(R) Platinum 8481C, 25 cores
- RAM: 150GB

Software :

- Operating System: Ubuntu 20.04 LTS
- Deep Learning Framework: PyTorch 1.12.1
- CUDA Version: 11.6